

University of Groningen

Improving the Region of Attraction of a Non-Hyperbolic Point in Slow-Fast Systems With One Fast Direction

Jardón Kojakhmetov, Hildeberto; Scherpen, Jacquélien M.A.

Published in:
IEEE Control Systems Letters

DOI:
[10.1109/LCSYS.2018.2832539](https://doi.org/10.1109/LCSYS.2018.2832539)

IMPORTANT NOTE: You are advised to consult the publisher's version (publisher's PDF) if you wish to cite from it. Please check the document version below.

Document Version
Final author's version (accepted by publisher, after peer review)

Publication date:
2018

[Link to publication in University of Groningen/UMCG research database](#)

Citation for published version (APA):

Jardón Kojakhmetov, H., & Scherpen, J. M. A. (2018). Improving the Region of Attraction of a Non-Hyperbolic Point in Slow-Fast Systems With One Fast Direction. *IEEE Control Systems Letters*, 2(2), 296-301. <https://doi.org/10.1109/LCSYS.2018.2832539>

Copyright

Other than for strictly personal use, it is not permitted to download or to forward/distribute the text or part of it without the consent of the author(s) and/or copyright holder(s), unless the work is under an open content license (like Creative Commons).

Take-down policy

If you believe that this document breaches copyright please contact us providing details, and we will remove access to the work immediately and investigate your claim.

Downloaded from the University of Groningen/UMCG research database (Pure): <http://www.rug.nl/research/portal>. For technical reasons the number of authors shown on this cover page is limited to 10 maximum.

Improving the region of attraction of a non-hyperbolic point in slow-fast systems with one fast direction

H. Jardón-Kojakhmetov¹ and Jacquélien M.A. Scherpen²

Abstract—Through recent research combining the Geometric Desingularization or blow-up method and classical control tools, it has been possible to locally stabilize non-hyperbolic points of singularly perturbed control systems. In this letter we propose a simple method to enlarge the region of attraction of a non-hyperbolic point in the aforementioned setting by expanding the geometric analysis around the singularity. In this way, we can synthesize improved controllers that stabilize non-hyperbolic points within a large domain of attraction. Our theoretical results are showcased in a couple of numerical examples.

Index Terms—Singular Perturbation methods, Slow-fast systems, Region of attraction, Nonlinear control systems.

I. INTRODUCTION

Singularly perturbed problems arise as models of e.g. nonlinear circuits and relaxation oscillators, biochemical oscillators, neuronal active potential, robotics, etc., in which two or more timescales are involved. In essence, a singular perturbation problem in Ordinary Differential Equations, also known as slow-fast system, can be regarded as a timescale separation between the states. Commonly, we assume that a system with such timescale separation can be treated by looking at the slow and the fast components independently. Then, from such information we can draw conclusions on the original system. A mathematical theory that supports the previous claim is due to Fenichel [1]. One of the many advantages of separating the behavior into slow and fast components is that it allows us to reduce the order of the models under study and that the so-called “composite control” can be implemented [2]–[8].

However, in order to have a valid separation into slow and fast components, we must assume a certain “regularity condition”. Technically, such condition requires that the fast subsystem must not have degenerate critical points (see Section II for more details). So, in the presence of degenerate singularities, the classical theory of singular perturbations and model order reduction techniques do not apply.

The main contribution of this letter is the improvement (by enlarging the region of attraction) of newly developed controllers that stabilize degenerate singularities of singularly perturbed control systems (see the details in Section III).

¹ H. Jardón-Kojakhmetov is with the faculty of mathematics of the Technical University of Munich, Boltzmannstr. 3, 85747 Garching b. Munich, Germany. e-mail: h.jardon.kojakhmetov@tum.de. ² Jacquélien M.A. Scherpen is with the Jan C. Willems Center for Systems and Control and the Engineering and Technology Institute of the University of Groningen, Nijenborgh 4, 9747 AG, Groningen, The Netherlands. e-mail: j.m.a.scherpen@rug.nl.

II. PRELIMINARIES

We study a class of slow-fast control systems (SFCSs) having one fast and an arbitrary number of slow variables given by

$$\begin{aligned} \dot{x} &= f(x, z, \varepsilon) + u(x, z, \varepsilon) \\ \varepsilon \dot{z} &= g(x, z, \varepsilon), \end{aligned} \quad (1)$$

where $x \in \mathbb{R}^{n_s}$, $z \in \mathbb{R}$, $0 < \varepsilon \ll 1$, $f(x, z, \varepsilon)$ and $g(x, z, \varepsilon)$ are smooth, and $u \in \mathbb{R}^{n_s}$ denotes the controller. Examples of this type of systems can be found in electrical circuits [9]–[11], biochemical oscillators [12], [13], etc. The independent time variable for (1) is t and therefore the over-dot stands for $\frac{d}{dt}$. When studying slow-fast systems one usually defines the fast-time variable $\tau = \frac{t}{\varepsilon}$, which allows to rewrite (1) as an ε -family of vector fields

$$X_\varepsilon : \begin{cases} x' &= \varepsilon (f(x, z, \varepsilon) + u(x, z, \varepsilon)) \\ z' &= g(x, z, \varepsilon), \end{cases} \quad (2)$$

where now the prime $'$ denotes derivative with respect to τ . Note that as long as $\varepsilon \neq 0$, the trajectories of (1) are equivalent to those of (2), the only difference is their time parametrization. An important geometric object in the study of slow-fast systems is the critical manifold.

Definition 1. *The critical manifold is defined as*

$$S = \{(x, z) \in \mathbb{R}^{n_s+1} \mid g(x, z, 0) = 0\}. \quad (3)$$

Note that, in the limit $\varepsilon \rightarrow 0$, the critical manifold is the phase-space of (1) and the set of equilibrium points of (2).

Remark 1. *In contrast to the classical setting (e.g. [6]), our main assumption is that the origin is a degenerate point of the critical manifold. Mathematically speaking this means that there exist a positive integer $k \geq 2$ such that $g(0, 0, 0) = \frac{\partial g}{\partial z}(0, 0, 0) = \dots = \frac{\partial^{k-1} g}{\partial z^{k-1}}(0, 0, 0) = 0$ and $\frac{\partial^k g}{\partial z^k}(0, 0, 0) \neq 0$. In the context of slow-fast systems, points $(x, z) \in \mathbb{R}^{n_s+1}$ where the previous holds are called non-hyperbolic.*

Remark 2. *Another important feature of (2) is that the control only actuates the slow variables. This is relevant in certain applications (see Section IV). Naturally, dealing with (2) is also more challenging than the fully actuated case. Briefly speaking, from a composite control perspective [6], the fast control can deal with the non hyperbolicity of the open-loop critical manifold.*

III. ENLARGING THE REGION OF ATTRACTION

Controllers that locally stabilize the origin of systems like (1) have been recently proposed in e.g. [14], [15]. These controllers deal with a class of singular perturbation problems for which the common regularity condition $\frac{\partial g}{\partial z}(x, z, 0) \neq 0$ does not hold. Here we propose an improvement to such controllers resulting on a larger region of attraction of the origin. Our main result is as follows (see a proof in Section V).

Theorem 1. Consider a slow-fast control system given by (1) and under the assumptions described above. Let the feedback controller $u(x, z, \varepsilon) = (u_1, \dots, u_{n_s})$ be given by

$$u = -f(0, 0, 0) + b\varepsilon^{\frac{-1}{2k-1}} z \hat{e}_1 - \varepsilon^{\frac{-k}{2k-1}} Ax + w, \quad (4)$$

where $b > 0$, $A \in \mathbb{R}^{n_s \times n_s}$ is a positive definite diagonal matrix, $\hat{e}_1 = [1, 0, \dots, 0]^\top \in \mathbb{R}^{n_s}$, and $w = (w_1, \dots, w_{k-1}, 0, \dots, 0) \in \mathbb{R}^{n_s}$ is given by

$$w_i = \begin{cases} 0 & z \geq 0 \\ -K_i (x_i (-z)^{i+1} + (-z)^{k+2} \eta_i^*) & z < 0 \end{cases}, \quad (5)$$

where $K_i \geq 0$, $\eta_i^* \in \mathbb{R}$ with $i = 1, \dots, k-1$. Then, if $K_i = 0$, the origin is locally asymptotically stable for $\varepsilon > 0$ sufficiently small. Furthermore, we can choose gains $K_i > 0$ and constants η_i^* that satisfy

$$1 - \sum_{i=1}^{k-1} (-1)^i \eta_i^* < 0 \quad (6)$$

such that for $\varepsilon > 0$ sufficiently small, the origin is rendered locally asymptotically stable, but its region of attraction is larger compared to the choice $K_i = 0$, $i = 1, \dots, k-1$.

Briefly speaking, Theorem 1 has two main components: first u , with $w = 0$, renders the origin locally asymptotically stable. Second, the term w captures trajectories that diverge and drives them towards a ‘‘safety zone’’¹ from which they can later converge towards the origin. We emphasize that w_i is continuous and differentiable at the origin.

IV. EXAMPLES

A. Didactic example

Let us consider the planar SFCS

$$\begin{aligned} \dot{x} &= 1 + u \\ \varepsilon \dot{z} &= -(z^2 + x) \end{aligned} \quad (7)$$

In Figure 1, we compare the performance of the controller (4) with $K = 0$ and $K > 0$. For this simulation we set the constants of Theorem 1 to $(A, b, K, \eta^*) = (1, 3, 10, -10)$. The first row of Figure 1 shows the open-loop dynamics, where the trajectories are quickly unbounded after crossing the non-hyperbolic origin. Next, in the second row of Figure 1 we show the dynamics of the closed-loop system with the controller proposed in Theorem 1 but with $K = 0$. Note that for $\varepsilon = 0.1$, two trajectories converge to and one diverges from the origin. However, when we decrease ε to $\varepsilon = 0.01$, only one trajectory converges while two diverge. Finally in the third row of Figure 1 we show the effect of the compensation proposed in Theorem

¹In fact, such safety zone is characterized by (6).

1, and note that the origin is asymptotically stable for both values of ε and within a large region of attraction compared to the case $K = 0$. In all these simulations we show trajectories with initial conditions $(x, z) = \{(-2, 2), (0, 2), (1, 2)\}$ in red, green and blue respectively.

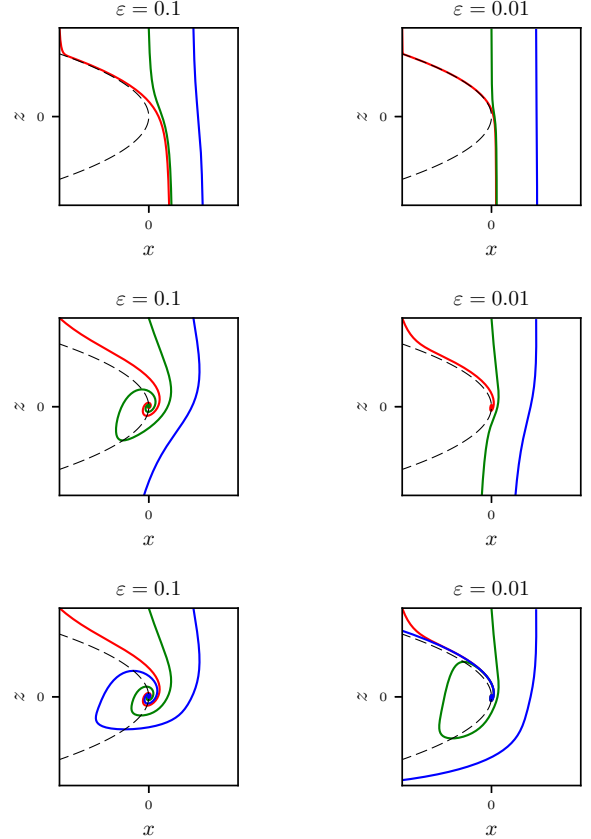


Fig. 1: Simulation of (7) with the controller of Theorem 1. In all plots, the dashed curve depicts the critical manifold $S = \{z^2 + x = 0\}$. The first row shows the open-loop dynamics, for which the origin is unstable. The second row shows the action of the controller of Theorem 1 with $K = 0$. The third row shows that the region of attraction of the origin has been enlarged due to the addition of w as in (5).

B. An electric circuit

We now exemplify the result of Theorem 1 with an electric circuit having a tunnel diode [11], [16] as shown in Figure 2a.

In [16] the diode’s constitutive relation is given by $I_D = V_D^3 - 9V_D^2 + 24V_D$, see Figure 2c. A parasitic capacitance is added to regularize the circuit, as shown in Figure 2b, see the justification in [9], [10]. It is assumed that the parasitic capacitance ε is much smaller than any other parameter of the circuit. The equations describing the regularized circuit are

$$\begin{aligned} \dot{V}_C &= \frac{1}{C} I_L \\ \dot{I}_L &= -\frac{1}{L} (V_C + V_D) \\ \varepsilon \dot{V}_D &= -(V_D^3 - 9V_D^2 + 24V_D - I_L), \end{aligned} \quad (8)$$

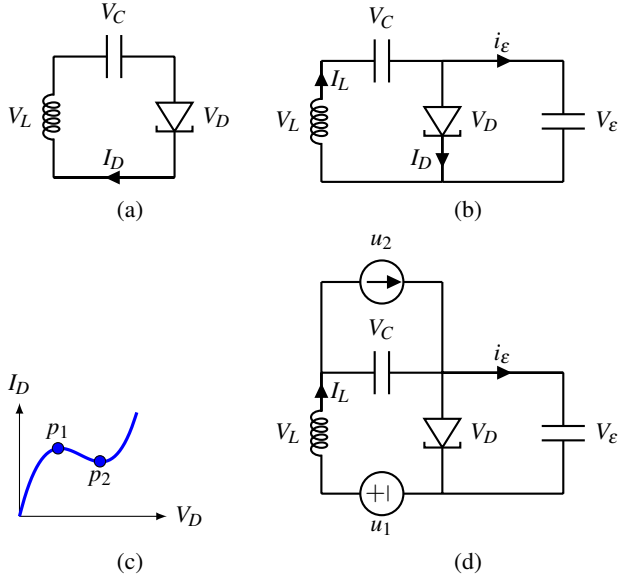


Fig. 2: (a) An electric circuit having a diode tunnel for negative resistance. (b) The characteristic curve of the tunnel diode. (c) Regularization of circuit (a). (d) The controlled circuit with voltage (u_1) and current (u_2) inputs.

where C and L stand respectively for the capacitor's and inductor's constants, V_D denotes the voltage across the tunnel diode, I_L is the current through the inductor, and V_C the voltage across the capacitor. It is straightforward to show that (8) has a unique equilibrium point at $p = (0, 0, 0)$, which is asymptotically stable. The critical manifold of (8) is precisely given by the constitutive relation $S = \{I_L = I_D = V_D^3 - 9V_D^2 + 24V_D\}$. Note that S has two fold points $p_1 = (V_D, I_D) = (2, 20)$ and $p_2 = (V_D, I_D) = (4, 16)$. The goal is to design a controller that stabilizes the operating point (V_C, I_L, V_D) at one of the fold points, say p_2 ². The desired value of V_C can be chosen arbitrarily but for simplicity we set it to $V_C = 0$. The controls are given by a voltage source (u_1) and a current source (u_2) as shown in Figure 2d, resulting in the model

$$\begin{aligned} \dot{V}_C &= \frac{1}{C}I_L - \frac{1}{C}u_2 \\ \dot{I}_L &= -\frac{1}{L}(V_C + V_D) + \frac{1}{L}u_1 \\ \varepsilon \dot{V}_D &= -(V_D^3 - 9V_D^2 + 24V_D - I_L). \end{aligned} \quad (9)$$

For the analysis, let us perform the following change of coordinates $(x_1, x_2, z) = (-I_L + 16, V_C, V_D - 4)$. Thus, the operating point $p_2 = (V_C, V_D, I_L) = (0, 4, 16)$ is translated to $(x_1, x_2, z) = (0, 0, 0)$. Then, we obtain

$$\begin{aligned} \dot{x}_1 &= \frac{1}{L}(x_2 + z + 4) - \frac{1}{L}u_1 \\ \dot{x}_2 &= \frac{1}{C}(16 - x_1) - \frac{1}{C}u_2 \\ \varepsilon \dot{z} &= -(3z^2 + x_1 + z^3), \end{aligned} \quad (10)$$

²Compare with [17] where a similar diode system is studied. In there the authors stabilize a *hyperbolic* operating point.

which is locally, near the origin, of the form studied in this paper. From Theorem 1 we choose u_1 and u_2 as

$$\begin{aligned} u_1 &= 4 + \varepsilon^{-\frac{2}{3}}a_1x_1 - b\varepsilon^{-\frac{1}{3}}z - w_1, \\ u_2 &= 16 + \varepsilon^{-\frac{2}{3}}a_2x_2. \end{aligned} \quad (11)$$

In Figures 3 and 4 we show simulations of (10)-(11) without and with the action of the compensation w_1 . We see that when $w_1 = 0$, not all trajectories converge to the desired equilibrium point, while convergence is achieved when w_i is implemented. For the simulation shown in Figures 3-4 we have chosen the parameters: $L = C = a_1 = a_2 = b = 1$, $\varepsilon = 0.01$. We show trajectories for two initial conditions: $(x_1, x_2, z) = (-10, 10, 3)$ and $(x_1, x_2, z) = (50, -30, -6)$. We let the system run in open-loop for the first 8.5 seconds. Then, at $t = 8.5$ we “turn on” the controllers.

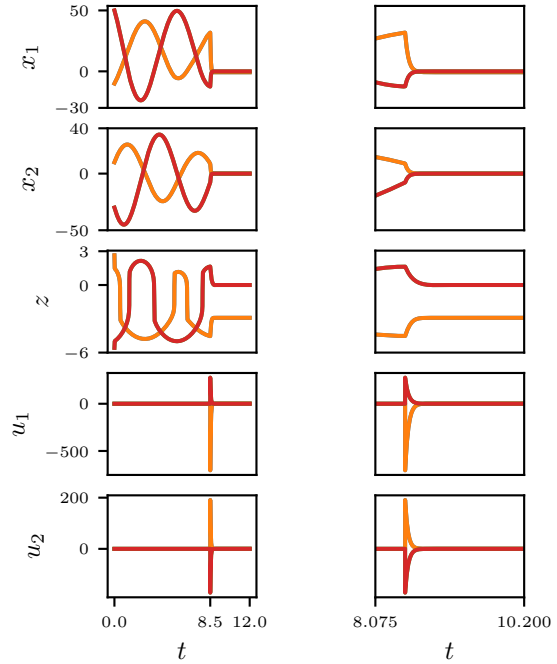


Fig. 3: Left: simulation of (10) with the controller (11) and with $w_1 = 0$. Note that in this case one of the trajectories converges to the origin while the other does not. Right: detail around $t = 8.5$ s.

V. PROOF OF THEOREM 1

The very first step is to find a local expression for the slow-fast control system under the given assumptions. From singularity theory and Malgrange's preparation theorem [18], [19], we know that the assumptions on the function $g(x, z, 0)$ allow us to write a local expression of the form

$$g(x, z, \varepsilon) = \pm \left(z^k + \sum_{i=1}^{k-1} x_i z^{i-1} \right) + O(\varepsilon). \quad (12)$$

The \pm sign has no important role in our analysis, and for convenience we choose the negative one (a similar analysis follows otherwise). On the other hand, we can also assume

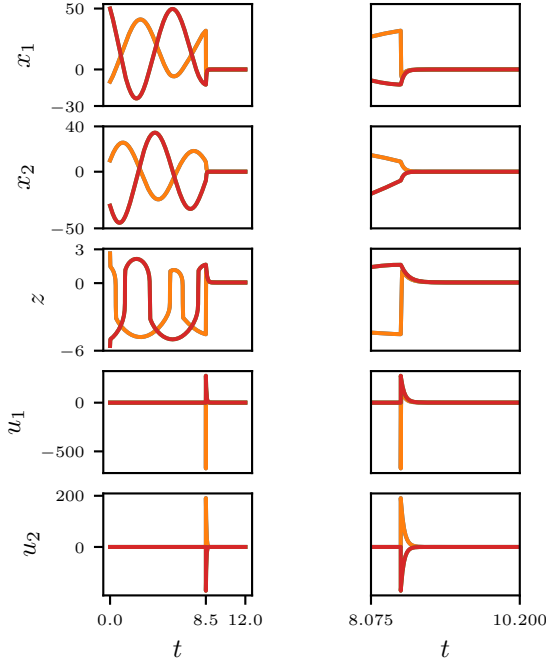


Fig. 4: Left: simulation of (10) with the controller (11) and with w_1 non-zero. For this simulation we have chosen $K_1 = 5$ and $\eta^* = -5$ as parameters of w_1 . Note that in contrast to Figure 3, we now have that both trajectories converge to the origin as desired. Right: detail around $t = 8.5$ s.

that $f(x, z, \varepsilon) = a + F(x, z) + O(\varepsilon)$, where $a = f(0, 0, 0)$ and $F(x, z)$ vanishes at the origin. So, in the rest of the proof we deal with the slow-fast control system

$$\begin{aligned} \dot{x} &= a + F(x, z) + u(x, z, \varepsilon) + O(\varepsilon) \\ \varepsilon \dot{z} &= - \left(z^k + \sum_{i=1}^{k-1} x_i z^{i-1} \right) + O(\varepsilon) \end{aligned} \quad (13)$$

The proof is based on the Geometric Desingularization method also known as blow-up [20], and common control techniques. We refer the reader to [20] for a general description of the method and to [14], [15], [21] for details on how the method works in the control systems setting. Briefly speaking, the idea is to use a generalized polar change of coordinates defined by

$$(r^\alpha \bar{x}, r^\beta \bar{z}, r^\gamma \bar{\varepsilon}) = (x, z, \varepsilon), \quad (14)$$

where $\bar{x} = (\bar{x}_1, \dots, \bar{x}_{n_s})$, $(\bar{x}, \bar{z}, \bar{\varepsilon}) \in \mathbb{S}^{n_s+1}$, that is $\sum_{i=1}^{n_s} \bar{x}_i^2 + \bar{z}^2 + \bar{\varepsilon}^2 = 1$, $r^\alpha \bar{x} = (r^{\alpha_1} \bar{x}_1, \dots, r^{\alpha_{n_s}} \bar{x}_{n_s})$, $\alpha = (\alpha_1, \dots, \alpha_{n_s}) \in \mathbb{N}^{n_s}$, $\beta \in \mathbb{N}$, $\gamma \in \mathbb{N}$, where $\mathbb{N}^{n_s} = \mathbb{N}^{n_s} \times \dots \times \mathbb{N}^{n_s}$ n_s -times. and $r \in [0, r_0)$ with $0 < r_0 < \infty$. Next, we study the vector field induced by such a change of coordinates, known as the blown up vector field. Since in general it is cumbersome to work with spherical coordinates, we often define charts that cover the sphere \mathbb{S}^{n_s+1} . Then, in each of such charts a local vector field is defined. The most important chart is the so called ‘‘central chart’’ defined by $K_{\bar{\varepsilon}} = \{\bar{\varepsilon} = 1\}$. The flow in $K_{\bar{\varepsilon}}$ is equivalent to that of the original system in a small neighborhood of the

origin. In this way, we shall be able to design a controller that locally stabilizes the origin of (13). Moreover, $K_{\bar{\varepsilon}}$ has a non-empty intersection with all other charts, which makes it ideal to investigate ways in which the region of attraction of the origin can be enlarged. The main novelty of this letter consists on further studying trajectories in another chart. As we explain below, for the class of systems studied here, trajectories diverge satisfying $z \rightarrow -\infty$. So, we shall also consider a local vector field in the chart $K_{-\bar{z}} = \{\bar{z} = -1\}$. It will be in such chart where we enlarge the region of attraction of the origin of (13).

Blown up vector field in the central chart:

The first step is to obtain a local vector field in the chart $K_{\bar{\varepsilon}}$. For this, let us propose a coordinate transformation defined by

$$\begin{aligned} (x_1, \dots, x_{k-1}, x_k, \dots, x_{n_s}, z, \varepsilon) &= \\ (\bar{r}^k \bar{x}_1, \dots, \bar{r}^2 \bar{x}_{k-1}, \bar{x}_k, \dots, \bar{x}_{n_s}, \bar{r} \bar{z}, \bar{r}^{2k-1}), \end{aligned} \quad (15)$$

where the weights of the map are chosen from the quasi-homogeneity of the function $g(x, z, 0)$ given in (12). Under the above change of coordinates we obtain

$$\begin{aligned} \bar{r}' &= 0 \\ \bar{x}'_i &= \bar{r}^{k+i-2} \left(a_i + \bar{F}_i(\bar{r}, \bar{x}, \bar{z}) + \bar{u}_i(\bar{r}, \bar{x}, \bar{z}) + O(\bar{r}^{2k-1}) \right) \\ \bar{x}'_j &= \bar{r}^{2k-1} \left(a_j + \bar{F}_j(\bar{r}, \bar{x}, \bar{z}) + \bar{u}_j(\bar{r}, \bar{x}, \bar{z}) + O(\bar{r}^{2k-1}) \right) \\ \bar{z}' &= -\bar{r}^{k-1} \left(\bar{z}^k + \sum_{i=1}^{k-1} \bar{x}_i \bar{z}^{i-1} + O(\bar{r}^{2k-1}) \right), \end{aligned} \quad (16)$$

where $i = 1, 2, \dots, k-1$ and $j = k, \dots, n_s$ and, for simplicity, \bar{u}_\bullet and \bar{F}_\bullet denote the components of the functions $u(x, z, 0)$ and $F(x, z, 0)$ under the proposed change of coordinates. That is, for example, $\bar{F}_\bullet(\bar{r}, \bar{x}, \bar{z}) = \bar{F}_\bullet(\bar{r}^k \bar{x}_1, \dots, \bar{r}^2 \bar{x}_{k-1}, \bar{x}_k, \dots, \bar{x}_{n_s}, \bar{r} \bar{z}, 0)$. We then see that $\bar{F}(0, \bar{x}, \bar{z}) = 0$ and $\bar{F}(\bar{r}, 0, 0) = 0$, the latter due to the fact that F does not depend on ε . Moreover, we also have $\frac{\partial \bar{F}_\bullet}{\partial \bar{x}_j} |_{\{\bar{r}=0\}} = \frac{\partial \bar{F}_\bullet}{\partial \bar{z}_j} |_{\{\bar{r}=0\}} = 0$. The previous properties will allow us to design simple linear feedback controllers as we now show. Note that (16) vanishes at $\bar{r} = 0$. So, we divide by \bar{r}^{k-1} obtaining an equivalent (for all $\bar{r} > 0$) vector field

$$\begin{aligned} \bar{r}' &= 0 \\ \bar{x}'_i &= \bar{r}^{i-1} (a_i + \bar{u}_i(\bar{r}, \bar{x}, \bar{z}) + O(\bar{r})) \\ \bar{x}'_j &= \bar{r}^k (a_j + \bar{u}_j(\bar{r}, \bar{x}, \bar{z}) + O(\bar{r})) \\ \bar{z}' &= - \left(\bar{z}^k + \sum_{i=1}^{k-1} \bar{x}_i \bar{z}^{i-1} + O(\bar{r}^{2k-1}) \right). \end{aligned} \quad (17)$$

Note that now, in contrast to (2), the limit $\bar{r} \rightarrow 0$ does not correspond to frozen \bar{x} variables. At this point, we could choose among the many control techniques to locally stabilize (17), but to keep the arguments simple, let us set

$$\begin{aligned} \bar{u}_i &= -a_i + \bar{r}^{1-i} (-A_i \bar{x}_i + b_i \bar{z}) + O(\bar{r}) \\ \bar{u}_j &= -a_j - \bar{r}^{-k} A_j \bar{x}_j + O(\bar{r}), \end{aligned} \quad (18)$$

where $A_i > 0$, $A_j > 0$ and $b_i > 0$ if $i = 1$ and $b_i = 0$ otherwise, for $i = 1, 2, \dots, k-1$ and $j = k, \dots, n_s$. Under this choice of controller the closed-loop system reads as

$$\begin{aligned} \bar{x}'_i &= -A_i \bar{x}_i + b_i \bar{z} + O(\bar{r}) \\ \bar{x}'_j &= -A_j \bar{x}_j + O(\bar{r}) \\ \bar{z}' &= -\left(\bar{z}^k + \sum_{i=1}^{k-1} \bar{x}_i \bar{z}^{i-1} + O(\bar{r}^{2k-1}) \right). \end{aligned} \quad (19)$$

Restricted to $\{\bar{r} = 0\}$, the Jacobian of (19) evaluated at the origin is of the form

$$J = \begin{bmatrix} -A & b_1 e_1 \\ -\bar{e}_1^\top & 0 \end{bmatrix}, \quad (20)$$

where $e_1 = (1, 0, \dots, 0)^\top \in \mathbb{R}^{n_s}$ and A is a $n_s \times n_s$ diagonal and Hurwitz matrix. It is straightforward to show that the eigenvalues of J are $\left\{ \frac{-A_1 \pm \sqrt{A_1^2 - 4b_1}}{2}, -A_2, \dots, -A_{n_s} \right\}$. From regular perturbation theory [22], we conclude that the origin of the closed loop system (19) is locally asymptotically stable for $\bar{r} \geq 0$ sufficiently small. Naturally, as we have used linearization and perturbation arguments to design the controller, the stability is only local. To obtain the first part of the controller of Theorem 1 we just blow down (return to the original coordinates via (15)) the leading order terms of (18) using (15), that is

$$u_i = -a_i + \left(b_i \varepsilon^{\frac{-i}{2k-1}} z - A_i \varepsilon^{\frac{-k}{2k-1}} x_i \right) \quad (21)$$

where $A_i > 0$ and $b_i > 0$ if $i = 1$ and $b_i = 0$ otherwise, for $i = 1, \dots, n_s$, and which in vector form can be written as in (4).

The idea of the rest of the proof is to introduce a term of order $O(\bar{r})$ in the controller, to enlarge the region of attraction of the origin. The motivation to do this can be seen in a simple example: let $k = 2$ and consider the following slow-fast system (left) and its corresponding closed-loop desingularization (right)

$$\begin{aligned} \dot{x} &= f(x, z, \varepsilon) + u & \bar{x}'_1 &= -a_1 \bar{x}_1 + b_1 \bar{z} \\ \varepsilon \dot{z} &= -(z^2 + x) & \bar{z}' &= -(\bar{z}^2 + \bar{x}_1) \end{aligned} \quad (22)$$

The phase portrait of the closed-loop desingularized system is shown in Figure 5.

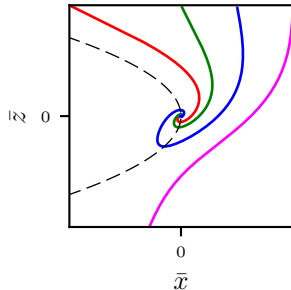


Fig. 5: Phase-portrait of the desingularized system in (22). Note that non-converging trajectories diverge with $\bar{z} \rightarrow -\infty$.

The situation presented above is particularly important for slow-fast control systems given by (13) with k even. The reason, apparent in Figure 5, is due to: i) for k even the critical manifold is “u-shaped” and ii) the term $-\bar{z}^k$ is dominant in the vertical direction, meaning that trajectories of (19) diverge with $\bar{z} \rightarrow -\infty$. Due to the previous observation, a good chart to look at to address this issue is $K_{-\bar{z}} = \{\bar{z} = -1\}$.

Blown up vector field in the chart $K_{-\bar{z}}$:

Now we study the slow-fast control system in the chart $K_{-\bar{z}}$. Roughly speaking, in this chart we are able to “see” how trajectories diverge towards $\bar{z} \rightarrow -\infty$ (equivalently $z \rightarrow -\infty$). The idea is to capture those trajectories, and drive them (via a controller) towards a “safety zone” from which they can then converge.

To avoid confusion between the coordinates of distinct charts, let us denote local coordinates in $K_{-\bar{z}}$ by

$$\begin{aligned} (x_1, \dots, x_{k-1}, x_k, \dots, x_{n_s}, z, \varepsilon) &= \\ (\bar{\rho}^k \bar{\eta}_1, \dots, \bar{\rho}^2 \bar{\eta}_{k-1}, \bar{\eta}_k, \dots, \bar{\eta}_{n_s}, -\bar{\rho}, \bar{\rho}^{2k-1} \bar{\mu}). \end{aligned} \quad (23)$$

It will be useful to know that the relationship between the coordinates of charts $K_{\bar{\varepsilon}}$ and $K_{-\bar{z}}$ reads as

$$\bar{\rho} = -\bar{r} \bar{z}, \quad \bar{\eta}_i = (-\bar{z})^{i-1-k} \bar{x}_i, \quad \bar{\eta}_j = \bar{x}_j, \quad \bar{\mu} = (-\bar{z})^{1-2k} \quad (24)$$

for $i = 1, \dots, k-1$, $j = k, \dots, n_s$, and $\bar{z} < 0$. Similarly,

$$\bar{r} = \bar{\rho} \bar{\mu}^{1/2k-1}, \quad \bar{x}_i = \bar{\mu}^{i-k-1/2k-1} \bar{\eta}_i, \quad \bar{x}_j = \bar{\eta}_j, \quad \bar{z} = -\bar{\mu}^{-1/2k-1} \quad (25)$$

for $i = 1, \dots, k-1$, $j = k, \dots, n_s$, and $\bar{\mu} > 0$. With the above relations we can transform (17)-(18) via (24) and (25) to obtain the blown up vector field in the chart $K_{-\bar{z}}$, which is given by

$$\begin{aligned} \bar{\rho}' &= \bar{\rho} U(\bar{\eta}) + O(\bar{\rho}^k \bar{\mu}) \\ \bar{\eta}'_i &= H_i + G_i + \bar{\rho}^{i-1} \bar{\mu} \bar{w}_i + O(\bar{\rho}^{k-1} \bar{\mu}) \\ \bar{\eta}'_j &= H_j + O(\bar{\rho}^{k-1} \bar{\mu}) \\ \bar{\mu}' &= -(2k-1) \bar{\mu} U_k(\bar{\eta}) + O(\bar{\rho}^{k-1} \bar{\mu}) \end{aligned} \quad (26)$$

where $\bar{w}_i = \bar{w}_i(\bar{\rho}, \bar{\eta}, \bar{\mu})$ and

$$\begin{aligned} H_i &= \bar{\rho}^{i-1} \bar{\mu} (\tilde{f}_i - a_i - \bar{\rho}^{1-i} (\bar{\mu}^{-\frac{i}{2k-1}} b_i + \bar{\mu}^{-\frac{k}{2k-1}} A_i \bar{\eta}_i)) \\ H_j &= \bar{\rho}^k \bar{\mu} (\tilde{f}_j - a_j - \bar{\rho}^{-k} \bar{\mu}^{-\frac{k}{2k-1}} A_j \bar{\eta}_j) \\ G_i &= -(k-i+1) U_k(\bar{\eta}) \bar{\eta}_i \end{aligned} \quad (27)$$

$$U_k(\bar{\eta}) = 1 - \sum_{i=1}^{k-1} (-1)^i \bar{\eta}_i.$$

with $\tilde{f}_\bullet = \tilde{f}_\bullet(\bar{\rho}, \bar{\eta}, \bar{\mu}) = f_\bullet(\bar{\rho}^\alpha \bar{\eta}, -\bar{\rho}, \bar{\rho}^{2k-1} \bar{\mu})$, where $\alpha = (k, k-1, \dots, 2)$. We have already substituted in (26) the controller expression (18). Furthermore, we are adding a controller term \bar{w}_i of order $O(\bar{\rho} \bar{\mu}^{1/2k-1}) = O(\bar{r})$, which shall be designed below. Note that by doing this we are not changing at all the local stability result already obtained in chart $K_{\bar{\varepsilon}}$. We emphasize that (26) is nothing more than (19) expressed in the coordinates of the chart $K_{-\bar{z}}$ and that all trajectories of (19) for $\bar{z} < 0$ are equivalent to trajectories of (26) for $\bar{\mu} > 0$. Now we have the following crucial observation.

Enlarging the region of attraction:

- 1) From the relations (24) and (25) we note that a trajectory of (26) satisfying $(\bar{\rho}(t), \bar{\eta}_i(t), \bar{\eta}_j(t), \bar{\mu}(t)) \rightarrow (0, 0, 0, \infty)$ corresponds to a trajectory in $K_{\bar{\varepsilon}}$ satisfying $(\bar{x}_i(t), \bar{x}_j(t), \bar{z}(t)) \rightarrow (0, 0, 0)$.
- 2) $\bar{z} \rightarrow -\infty$ implies $\bar{\mu} \rightarrow 0$.
- 3) If $U_k(\bar{\eta}) < 0$ then $\bar{\rho} \rightarrow 0$ and $\bar{\mu} \rightarrow \infty$.

Remark 3. For k even (the important case for enlarging the region of attraction), the condition $U_k(\bar{\eta}) < 0$ is equivalent to points “inside the critical manifold”. In other words, points in $K_{-\bar{z}}$ where $U_k(\bar{\eta}) < 0$ correspond to points in $K_{\bar{\varepsilon}}$ where $\bar{z}^k + \sum_{i=1}^{k-1} \bar{x}_i \bar{z}^{i-1} < 0$. In Figure 5, see also the third row of Figure 1 this corresponds to points inside the parabola. Note that once there, the trajectories are attracted towards the upper branch of the parabola. Again, this scenario is similar for any k even.

To design \bar{w}_i we shall use “high-gain” arguments. Although more complicated controllers can be designed, we want to keep the arguments as simple as possible to showcase the technique rather than the design itself. Thus, we propose $\bar{w} = -K\bar{\rho}^q(\bar{\eta} - \bar{\eta}^*)$, where $K > 0$ is diagonal, $\bar{\eta}^*$ satisfies $U_k(\bar{\eta}^*) < 0$ and the integer $q > 1$ shall be set later. Note then that for $\bar{\rho} > 0$, $\bar{\mu} > 0$ and some large $K > 0$, the point $\bar{\eta}^*$ is attracting and $\bar{\rho} \rightarrow 0$.

In essence, what \bar{w}_i does is it captures the trajectories that diverge with $\bar{z} \rightarrow -\infty$ and forces them to approach the safety zone $U_k(\bar{\eta}^*) < 0$. To obtain the expression of w in (5) we just blow down using the expressions $\bar{\rho} = -z$ and $\bar{\eta}_i = x_i(-z)^{-k+i-1}$. Therefore

$$w_i = -K_i(-z)^q \left(x_i(-z)^{-k+i-1} - \bar{\eta}_i^* \right). \quad (28)$$

We choose now q such that $w_i(0, 0) = \frac{\partial w_i}{\partial z}(0, 0) = 0$, which is satisfied if $q > k + 1$. For simplicity we choose $q = k + 2$ so that the final expression of the controller is

$$w_i = -K_i \left(x_i(-z)^{i+1} + (-z)^{k+2} \bar{\eta}_i^* \right), \quad (29)$$

which is as stated in (5). Furthermore, note that our analysis in chart $K_{-\bar{z}}$ is only valid in the subspace $\{z < 0\}$. This is the reason to propose the “compensation” w_i as in (5). Finally, it is straightforward to check that w_i is indeed of order $O(\bar{\rho})$ in chart $K_{\bar{\varepsilon}}$ meaning that it does not change the local stability result obtained at the beginning of the proof.

VI. CONCLUSIONS

We have presented a novel method to improve the region of attraction of a non-hyperbolic point of a slow-fast control system. The main difficulty of stabilizing such type of points is that the well known singular perturbation control techniques [6] cannot be employed in such setting. The main tool that we use is the Geometric Desingularization method [20], [23]. With such technique it is possible to locally desingularize the system and then propose simple controllers to render a non-hyperbolic point asymptotically stable. The important contribution of this paper is to use in a greater extent the Geometric Desingularization method to enlarge the region of attraction of the non-hyperbolic point. In essence, we look at an appropriate chart where the trajectories that diverge from the origin can be handled and driven (via an extra term in the controller)

towards a zone from where they can later converge to the origin. There are still challenging open questions to address from which we point out: rigorous estimates on the size of the region of attraction can be important for applications and should be investigated. Similarly, the effects of the higher order terms (that we disregard in the blow-up analysis) and of other disturbances is also of interest.

REFERENCES

- [1] N. Fenichel, “Geometric singular perturbation theory for ordinary differential equations,” *Journal of Differential Equations*, vol. 31, no. 1, pp. 53–98, 1 1979, doi: 10.1016/0022-0396(79)90152-9.
- [2] A. C. Antoulas, D. C. Sorensen, and S. Gugercin, “A survey of model reduction methods for large-scale systems,” *Contemporary mathematics*, vol. 280, pp. 193–220, 2001.
- [3] J. H. Chow, *Power system coherency and model reduction*. Springer, 2013.
- [4] H. Jardón-Kojakhmetov, M. Muñoz-Arias, and J. M. Scherpen, “Model reduction of a flexible-joint robot: a Port-Hamiltonian approach,” *IFAC-PapersOnLine*, vol. 49, no. 18, pp. 832–837, 2016, doi: 10.1016/j.ifacol.2016.10.269.
- [5] B. Siciliano and W. J. Book, “A singular perturbation approach to control of lightweight flexible manipulators,” *The International Journal of Robotics Research*, vol. 7, no. 4, pp. 79–90, 1988.
- [6] P. V. Kokotovic, H. K. Khalil, and J. O’Reilly, *Singular Perturbation Methods in Control: Analysis and Design*. Orlando, FL, USA: Academic Press, Inc., 1986.
- [7] A. Kumar, P. D. Christofides, and P. Daoutidis, “Singular perturbation modeling of nonlinear processes with nonexplicit time-scale multiplicity,” *Chemical Engineering Science*, vol. 53, no. 8, pp. 1491–1504, 1998.
- [8] R. Marino and P. V. Kokotovic, “A geometric approach to nonlinear singularly perturbed control systems,” *Automatica*, vol. 24, no. 1, pp. 31–41, 1988.
- [9] E. Ihrig, “The regularization of nonlinear electrical circuits,” *Proceedings of the American Mathematical Society*, pp. 179–183, 1975.
- [10] S. Smale, “On the mathematical foundations of electrical circuit theory,” *Journal of Differential Geometry*, vol. 7, no. 1-2, pp. 193–210, 1972.
- [11] F. Takens, “Constrained Equations: a Study of Implicit Differential Equations and their Discontinuous Solutions,” in *Structural Stability, the Theory of Catastrophes, and Applications in the Sciences*, ser. LNM 525. Springer-Verlag, 1976, pp. 134–234.
- [12] I. Kosiuk and P. Szmolyan, “Scaling in singular perturbation problems: blowing up a relaxation oscillator,” *SIAM Journal on Applied Dynamical Systems*, vol. 10, no. 4, pp. 1307–1343, 2011.
- [13] —, “Geometric analysis of the goldbeter minimal model for the embryonic cell cycle,” *Journal of mathematical biology*, vol. 72, no. 5, pp. 1337–1368, 2016.
- [14] H. Jardón-Kojakhmetov and J. M. A. Scherpen, “Stabilization of a planar slow-fast system at a non-hyperbolic point,” in *22nd International Symposium on Mathematical Theory of Networks and Systems*, 2016.
- [15] H. Jardón-Kojakhmetov, J. M. Scherpen, and D. del Puerto-Flores, “Nonlinear adaptive stabilization of a class of planar slow-fast systems at a non-hyperbolic point,” in *American Control Conference (ACC), 2017*. IEEE, 2017, pp. 2441–2446.
- [16] G. Reissig, “Differential-algebraic equations and impasse points,” *IEEE Transactions on Circuits and Systems I: Fundamental Theory and Applications*, vol. 43, no. 2, pp. 122–133, Feb 1996.
- [17] E. García-Canseco, D. Jeltsema, R. Ortega, and J. M. A. Scherpen, “Power-based control of physical systems,” *Automatica*, vol. 46, no. 1, pp. 127 – 132, 2010.
- [18] V. I. Arnold, V. V. Goryunov, O. V. Lyashko, A. Iacob, and V. A. Vasil’ev, *Singularity Theory: I*, ser. Encyclopaedia of mathematical sciences. Springer Berlin Heidelberg, 1998, no. VI.
- [19] M. Golubinsky and V. Guillemin, *Stable Mappings and their Singularities*. Springer-Verlag, 1973.
- [20] C. Kuehn, *Multiple Time Scale Dynamics*. Springer, 2015.
- [21] H. Jardón-Kojakhmetov, J. M. A. Scherpen, and D. del Puerto-Flores, “Stabilization of slow-fast systems at fold points,” preprint arXiv:1704.05654, 2017.
- [22] J. A. Murdock, *Perturbations: theory and methods*. SIAM, 1999, vol. 27.
- [23] F. Dumortier and R. H. Roussarie, *Canard cycles and center manifolds*. American Mathematical Soc., 1996, vol. 577.